D.O. KHARCHENKO, V.O. KHARCHENKO, A.I. BASHTOVA

Institute of Applied Physics, Nat. Acad. of Sci. of Ukraine
(58, Petropavlivska Str., Sumy 40000, Ukraine; e-mail: dikh@ipfcentr.sumy.ua)

PACS 05.40.-a, 61.72.-y,
81.16.Rf

SIMULATION OF A SPATIAL ORGANIZATION OF POINT DEFECTS IN IRRADIATED SYSTEMS

In the framework of rate theory, a generalized statistical approach has been proposed to describe the spatial organization of point defects of the vacancy type into clusters and pores in irradiated systems. The approach makes allowance for the generation of point defects by elastic fields, as well as for defect interaction. The model is applied to study the defect pattern formation in pure nickel. The conditions required for the pattern formation at actual irradiation regimes in reactors have been analyzed. The peculiarities of microstructure changes at various temperatures and dose accumulation rates have been obtained both analytically and numerically. The defect pattern period and the change of a characteristic pattern size have been studied by applying the statistical methods to analyze the obtained numerical data. The results are in good correspondence with well-known experimental observations of the defect microstructure formation in irradiated materials under reactor conditions.

K e y w o r d s: rate theory, spatial organization of point defects of the vacancy type, clusters, pores, irradiated systems, defect pattern formation, irradiation in reactors, numerical simulation.

1. Introduction

It is well known that the influence of high-energy particles on and, in general, irradiation of solids give rise to variations in the structural-phase states of the latter. Changes in the physical and mechanical properties of such systems are driven by the process of defect formation in the crystalline structure and the spatial organization of arisen defects, which results in certain microstructural transformations. As such, the formation of vacancy clusters (di-, three-, and tetra-vacancies) [1], individual pores and their lattices [2, 3], precipitates, and defect walls [4], the orderings of vacancy loops [5, 6] can be mentioned. The majority of defects formed owing to an external influence are thermodynamically unstable. Consequently, their uniform distribution becomes also unstable, which results in their spatial reorganization: an effective reduction of system's entropy takes place as a result of the self-organization induced by external factors. In general, such processes in condensed systems are challenging and interesting not only from the theoretical viewpoint. For the systems of defects in solids, those problems attract a special attention, because knowing the behavior of

such statistical ensemble allows the mechanisms of microstructural transformations in irradiated materials to be revealed and analyzed. Moreover, they are useful when forecasting the behavior of pure substances and alloys. Therefore, this work is aimed at studying the processes of micropattern formation in constructional materials (nickel is taken as an example), provided that point defects become organized as a result of the constant irradiation action under reactor conditions.

From literature data (see, e.g., work [7]), it is known that, in the case of low-energy incident particles (their energy does not exceed very much the energy of an initially knocked out atom; for example, $E_d \approx 30$ eV for nickel), isolated Frenkel pairs are formed. If the energy of incident particles is high (for example, it exceeds $2E_d$), the cascades of displacements are formed. The minimum energy of nickel ions required to initiate the process of defect formation in nickel itself does not exceed 60 eV; this quantity amounts to 250 eV for α-particles, to 860 eV for neutrons, and to 800 keV for electrons. From experimental observations, it was found that the formation of organized defect pattern demands that defects should be produced in cascades. Such processes are mainly observed under ion and neutron irradiation [8]. Spatial defect patterns were also
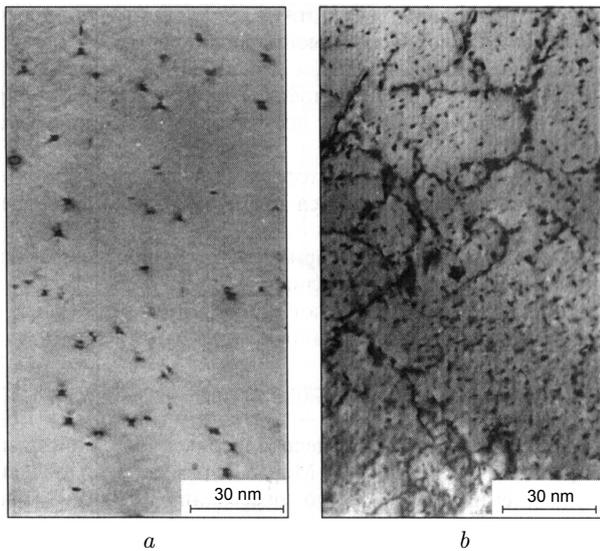
Fig. 1. Microstructure of chrome-nickel steel (*a*) and pure nickel (*b*) irradiated with Ni ions at room temperature to doses of 40 d.p.a (*a*) and 20 d.p.a (*b*). Taken from work [11]

observed at laser irradiation with pulse intensities $I \sim 10^7 \div 10^8$ W/cm^2, when the shock wave formed defects in the bulk of a solid, where the wave front had propagated [9, 10]. It should be noted that, at moderate intensities ($I \sim 10^4 \div 10^7$ W/cm^2) and in the absence of a shock wave, the thermal mechanism of defect formation plays the dominant role. The corresponding concentration of nonequilibrium point defects can exceed the equilibrium one by several orders of magnitude [9].

The rate of defect formation that characterizes irradiation conditions (in reactors or on accelerators) is determined by the number of displaced atoms, the spectral density of a particle flux, and the defect formation cross-section. It is known that, in the case of irradiation in reactors, this quantity has an order of magnitude of 10^{-6} d.p.a/s (displacement per atom per second); in the case of accelerators, we have an estimate of 10^{-3} d.p.a/s. At the irradiation with laser pulses, this quantity will evidently be substantially lower than the reactor one. It should be noted that the temporal scale for the running of corresponding processes in crystalline systems is as follows: about 10^{-16} s for the formation of a primarily knocked out atom and about 10^{-13} s for passing the cascade; the relaxation (annealing) stage runs within an interval of 10^{-8}–10^{-7} s.

The spatial scales of defect organization also differ considerably. Here, besides the diffusion length, one has to consider the nanometer ranges of the defect interaction and the peculiarities in the formation of vacancy nanoclusters. For instance, the defect clusters 5.5 nm in average size were observed while irradiating Ni and Cu targets with 3-MeV protons to doses below 2 d.p.a [1]. At low doses (0.01 d.p.a), defects were distributed uniformly. At the same time, at doses higher than 0.1 d.p.a, fluctuations of defect clusters transformed into pronounced and periodically arranged clusters with a period of 20–30 nm. Patterns typical of the formation of small defect clusters ("black dots") in stainless steel and pure nickel are depicted in Fig. 1. The number of "black dot" clusters in stainless steels was found to amount to 1% of all defects, whereas the concentration of vacancy tetrahedra for Ni and Cu ranged from 25 to 50% [11]. Similar effects were observed for Mo, Al, Nb, Ta, W, and Ti –Zr–Mo alloys with a periodic (a period of 200–800 Å) arrangement of pores 20–100 Å in dimensions.

Since the behavior of such systems is determined by wide spatial and temporal intervals, the theoretical researches of a micropattern formation use approaches that include the consideration at various hierarchical description levels: from the quantum mechanical theory to numerical methods (e.g., the finite-element method) while studying a constructional element fabricated from a given material. The research of the defect formation processes at the microscopic level is carried out taking advantage of molecular dynamics methods, whereas the approaches based on the Monte Carlo [12–14] and phase field [15] techniques are well suitable for diffusion time intervals.

The application of a specific modeling method at every level of consideration does not allow the influence of the lower and upper hierarchical levels to be taken into account. Therefore, the application of hybrid techniques or the development of existing approaches to make allowance for such an influence is one of the solutions of this problem. As a hybrid method, we may regard the method of the crystal phase field, which adequately describes the behavior of an atomic system in terms of atomic concentrations [16, 17]. It was successfully used to study the diffusion of defects [18], the dislocation dynamics [19], and structural transformations [20–23]. This approach is effectively used while describing and simulating the

formation of surface structures in the course of ionic sputtering (see, e.g., works [24, 25]). The generalization of the Cahn–Hilliard theory under an assumption that there exist two temporal scales (the diffusion time and the time of cascade passage) allows the processes of precipitate emergence and binary system stratification at irradiation to be analyzed (see, e.g., works [26–28]). At the mesoscopic level, the dynamics of defects can be presented in the framework of rate theory by considering the behavior of point defects and their diffusion and interaction [29, 30]. It allows one not only to describe the quantitative characteristics of defects and the swelling effect, but also to explain the spatial organization of defects at the formation of their clusters, pores, and extended defects (pore walls); the formation of grain boundaries; and the outcrop of defects on them [31].

In this work, on the basis of the developed rate theory, which involves the interaction between point defects, the processes of the vacancy-type defect cluster formation are studied assuming that interstitial atoms move quickly and quickly arrive at sinks. Nickel, the most wide-spread constructional material used in the atomic engineering, was selected as a system to study. We will demonstrate that, if the processes of defect generation by the elastic field of defects themselves are taken into account, the existence of bistable stationary states in this system becomes possible. We will analyze the types of defect patterns and determine the conditions of their realization for various rates of defect formation and irradiation temperatures. The deterministic mesoscopic model developed in this work will be generalized by taking the fluctuation contribution into consideration that simulates the influence of the microscopic level in accordance with the fluctuation-dissipation theorem. The fluctuation effect obtained at the formation of stationary defect patterns will be analyzed. In order to generalize the results obtained, the rate of defect formation is chosen within the interval ranging from the values corresponding to laser irradiation to those that are characteristic of accelerators.

The structure of the paper is as follows. In Section 2, the model of interacting point defects is developed. In Section 3, the stability of stationary states is analyzed in the linear approximation. In Section 4, the deterministic approach is generalized to the case where the action of an internal stochastic source is taken into account. In Section 5, the formation of stationary defect patterns in a nonlinear system is examined. Section 6 contains the results of the numerical simulation of the pattern formation dynamics. Conclusions are summarized in the last section of the paper.

2. Model of a Point-Defect System

In the framework of approaches inherent to the rate theory, the dynamics of radiation-induced defects–as such, we will regard only point-like ones (vacancies and interstitial atoms)–is described by equations that look like

$$\partial_t c_v = K(1-\varepsilon_v) - D_v S_v (c_v - c_{0v}) - \alpha c_i c_v - \nabla \cdot \mathbf{J}_v^0,$$
$$\partial_t c_i = K(1 - \varepsilon_i) - D_i S_i c_i - \alpha c_i c_v - \nabla \cdot \mathbf{J}_i^0. \tag{1}$$

Here, $c_{v,i}$ are the concentrations of vacancies (the subscript v) and interstitial atoms (the subscript i); $c_{0v} = e^{-E_v^f/T}$ is the equilibrium concentration of vacancies expressed in terms of their formation energy E_v^f and the temperature T measured in the energy units; K is the rate of dose accumulation; $\varepsilon_{v,i}$ are the intensities of cascade collapse at the formation of the loops of vacancies and interstitial atoms ($\varepsilon_v \gg \varepsilon_i$); and $D_{v,i} = D_{v,i}^0 e^{-E_{v,i}^m/T}$ are the diffusion coefficients of vacancies and interstitial atoms, which are determined by the corresponding preexponential factors $D_{v,i}^0$ and the defect migration energies $E_{v,i}^m$. The sink intensities $S_{v,i}$ for point defects of two types are determined by the density of a dislocation grid ρ_N and the densities of vacancy and interstitial loops $\rho_{v,i}$ with the preference $Z_{\{\cdot,\cdot\}}$. The general expression for the sink intensities looks like $S_{v,i} = Z_{\{v,i\}N}\rho_N + Z_{\{v,i\}V}\rho_v + Z_{\{v,i\}I}\rho_i$, where $Z_{vN} = Z_{vI} = Z_{vV} = 1$, $Z_{iN} = 1 + B$, $Z_{iI} \simeq Z_{iV} \simeq 1 + B'$, $B' \geq B$, and $B \approx 0.1$. The recombination of point defects is given by the coefficient $\alpha = 4\pi r_0(D_i + D_v)/\Omega$, where r_0 is the defect interaction radius, and Ω the atomic volume. Since defects are mobile particles of the micropattern, the evolution equations for their concentrations involve a contribution of the diffusion fluxes denoted as $\mathbf{J}_v^0$ and $\mathbf{J}_i^0$, respectively.

When changing to dimensionless variables, we can use the definitions

$$S_{v,i} = Z_{\{v,i\}N}\rho_N(1 + \rho_v^* + \rho_i^*), \quad \rho_{v,i}^* \equiv \rho_{v,i}/\rho_N, \tag{2}$$

where $t' \equiv t\lambda_v$ stands for the temporal variable, with $\lambda_v \equiv D_v Z_{vN}\rho_N$; the rescaled defect concentrations $x_{i,v} = \gamma c_{i,v}$ are determined by the parameter

$\gamma \equiv \alpha/\lambda_v$; and $P \equiv \gamma K/\lambda_v$ is a function of the dose accumulation rate and the temperature measured in terms of d.p.a units. Using the notation $\mu \equiv (1 + \rho_v^* + \rho_i^*)$ and $Z_{iN}/Z_{vN} = 1 + B$ and adopting that the diffusion coefficients for vacancies and interstitial atoms differ from each other by several orders of magnitude, it is possible to introduce the small parameter $D_v/D_i \equiv \epsilon \ll 1$, which describes the difference between the time intervals of evolution for defects of two types. Then, we arrive at a system of differential equations

$$\partial_t x_v = P(1 - \varepsilon_v) - \mu(x_v - x_{0v}) - x_i x_v - \nabla \cdot \mathbf{J}_v;$$
$$\epsilon \partial_t x_i = \epsilon P(1 - \varepsilon_i) - (1 + B)\mu x_i - \epsilon x_i x_v - \epsilon \nabla \cdot \mathbf{J}_i, \quad (3)$$

where $\mathbf{J}_{i,v} \equiv \gamma \mathbf{J}_{i,v}^0/\lambda_v$. From whence, it follows that the concentration of interstitial atoms is a quickly changing variable in comparison with that of vacancies and, hence, can be effectively neglected in the adiabatic approximation. Really under the condition $\epsilon \partial_t x_i \approx 0$, we obtain the following expression for the concentration of interstitial atoms:

$$x_i = P(1 - \varepsilon_i)/[(1 + B)\mu/\epsilon + x_v].$$

If this quantity is substituted into the first equation of system (3), the dynamics of the system is described by the equation of slow mode evolution, $x \equiv x_v$.

It should be noted that the defect formation has a thermofluctuation character. Its probability grows with the temperature (the irradiation intensity) and the defect concentration [9]. As was shown in work [10], the latter phenomenon is connected with a change in the height of an activation barrier for the defect formation, which occurs owing to the elastic deformation of the medium induced by the defects themselves. In this case, in order to take the mentioned effect into account, the evolution equation for x has to be appended by a term describing the defect generation according to that mechanism. The corresponding term looks like $G \exp(-E/T)$, where $G = p\omega_D\gamma/\lambda_v$ is the frequency factor determined in terms of the Debye frequency ω_D, $p \approx 10^{-6}$ is the probability to realize this process, and $E = E_m^f + E_v^m - E^e(\bar{r})$ is the activation energy, which decreases due to the action of the deformation field $E^e(\bar{r})$ created by the defects. Supposing that the relation between the average defect-to-defect distance and the defect concentration has the form $\bar{r} = x^{-1/3}$ and following the results of work [10], this term looks like

$G \exp(\varepsilon x/(1 + x^2))$, where the parameter $\varepsilon \equiv 2ZE_0^e/T$ depends on the characteristic energy of the deformation field E_0^e and the coordination number Z. This contribution to the defect dynamics is substantial at laser irradiation intensities (at small rates of dose accumulation). Therefore, despite that it is small at a particle irradiation owing to the cascade mechanism of defect formation, we hold it in the subsequent consideration without loss of generality.

Consider now the diffusion flux of vacancies. As a whole, it includes the Fickian component $-L_d^2 \nabla x$ with the diffusion length $L_d^2 \equiv D_v/\lambda_v$ and a component describing the interaction between defects. In the case of a stationary flux, we obtain

$$\mathbf{J} = -L_d^2 \nabla x + \mathbf{v} x. \quad (4)$$

Here, the second component describes the motion of defects at the rate $\mathbf{v} = (L_d^2/T)\mathbf{F}$ under the action of a force $\mathbf{F} = -\nabla U$ invoked by the defect interaction. The flux $\mathbf{J}$ can be rewritten in the canonical form $\mathbf{J} = -L_d^2 M(x)\nabla \mu(x)$, where $M(x) = x$ is the mobility, and $\mu(x) = \delta\mathcal{F}/\delta x$ plays the role of chemical potential. Then, the corresponding free energy functional looks like

$$\mathcal{F} = \int d\mathbf{r} f(x(\mathbf{r})) - \frac{1}{2T} \int d\mathbf{r} \int d\mathbf{r}' x(\mathbf{r})\tilde{u}(\mathbf{r}, \mathbf{r}')x(\mathbf{r}'). \quad (5)$$

Here, the free energy density $f(x) = x(\ln x - 1)$ in the first term describes the gas of free particles, the second term characterizes pair interactions in the self-consistent approximation [31–33], and $-\tilde{u}(r)$ is the attractive potential between two particles (defects) separated by the distance r. The function $\tilde{u}(r)$ is selected symmetric in a vicinity of the defect, $\int \tilde{u}(r)r^{2n+1}dr = 0$. If the field $x(r)$ does not change considerably over the defect interaction distance $r_0 \simeq \Omega^{1/3}$, we may use a series expansion up to the second non-disappearing term, i.e.

$$\int d\mathbf{r}'\tilde{u}(\mathbf{r} - \mathbf{r}')x(\mathbf{r}') \approx \varepsilon(x + r_0^2\nabla^2 x). \quad (6)$$

The first term on the left-hand side of Eq. (6) gives rise to a standard relation between the elastic field potential $U = -\int d\mathbf{r}'\tilde{u}(\mathbf{r} - \mathbf{r}')x(\mathbf{r}')$ and x in the framework of elasticity theory. Really, the potential U is connected with the displacement vector $\mathbf{u}$ by the formula $U = -\kappa\varpi\nabla \cdot \mathbf{u}$, where $\nabla \cdot \mathbf{u} \propto \varpi x$, κ is the bulk modulus, and ϖ is the dilatation parameter [9].

Therefore, the expression for the effective flux looks like $\mathbf{J} \propto -(1 - \varpi^2\kappa x/T)\nabla x$. The second term in expansion (6) characterizes microscopic processes of interaction between defects at the distance of correlation (interaction) length r_0. Under normal conditions, this term can be omitted because its contribution is small in comparison with the diffusion one. Substituting Eq. (6) into definition (4) for the total flux, one can see that even if the first term in Eq. (6) is taken into account, the expression for the diffusion flux will include the coefficient $(1 - \varepsilon x)$ dependent on the concentration field, i.e. $\mathbf{J} \propto -(1 - \varepsilon x)\nabla x$. This coefficient can change its sign depending on x. As a result, we obtain a divergence, which means that a uniform distribution of vacancies becomes unstable if the rate of their formation exceeds a critical value determined by the temperature, sink concentration, and volume dilatation. The appearance of this directed flux results in the vacancy oversaturation and the formation of defect patterns such as pores and so forth. From the mathematical viewpoint, this divergence cannot be compensated by non-linearities in the evolution equation [31–33]. It can be prevented only by making allowance for the second (interaction) component in expansion (6). Therefore, this component must be retained in the subsequent consideration. As will be demonstrated below, it is this component that characterizes the dimensions of defect patterns.

Hence, if all the features indicated above are taken into account, the general expression for the model concerned is given by an equation of the reaction-diffusion type,

$$\partial_t x = R(x; K, T) - \nabla \cdot \mathbf{J}, \tag{7}$$

where the full expressions for the reaction component and the flux look like, respectively,

$$R(x; K, T) \equiv P(K, T)(1 - \varepsilon_v) - \mu(x - x_0) -$$

$$-\frac{P(K, T)(1 - \varepsilon_i)x}{\frac{\mu(1+B)}{\epsilon} + x} + G(T)e^{\frac{\varepsilon x}{1+x^2}},$$

$$\mathbf{J}(x; T) \equiv -\left[\nabla x - \varepsilon(T)x\nabla(x + \ell^2\nabla^2 x)\right]. \tag{8}$$

Here, the rescaling of the spatial variable $\mathbf{r}' = \mathbf{r}/L_d$ is taken into account, and the dimensionless length $\ell \equiv r_0/L_d$ is introduced.

For the further consideration, let us use the data set for pure nickel [8] (see Table 1). The estimation of the

diffusion length gives $L_d \simeq 10^{-6} \div 10^{-7}$ m, whereas $\ell \ll 1$. The rate of dose accumulation amounts to $K \simeq 10^{-6}$ d.p.a/s for reactors and $K \simeq 10^{-3}$ d.p.a/s for accelerators. At laser irradiation, the dose accumulation rate is several orders of magnitude lower than that for reactors and depends on the power of laser pulses.

3. Analysis of the Linearized System Stability

Consider firstly a uniform system in the stationary case, $t \to \infty$. Then its stationary states x_s are given by the solutions of the equation $\partial_t x = 0$. The corresponding dependences are shown in Fig. 2, *a* for various fixed temperatures and various values p of the probability of vacancy generation by the field of elastic stresses. As is seen from Fig. 2, *a*, without an elastic field ($p = 0$), the concentration of vacancies monotonously increases from the equilibrium value c_{0v} by several orders of magnitude even at doses lower than 1 d.p.a. However, in the case of non-zero p-value, the dependence $c_v(K)$ demonstrates a hysteretic behavior, which means the appearance of a bimodality for the stationary states. This peculiarity manifests itself at low doses or low rates of defect formation typical of the laser irradiation. It can also reveal itself at additional mechanical loadings that raise the energy level E_0^e. At low and high doses, the stationary dependences coincide well with those for the case $p = 0$. From the physical viewpoint, such a behavior can evidently be explained as follows. Proceeding from the equilibrium concentration $c_{0v} = c_v(K = 0, T)$, as growth of the irradiation dose

Basic material parameters for nickel

Parameter	Value	Measurement unit
E_v^f	1.8	eV
E_v^m	1.04	eV
E_i^m	0.3	eV
E_0^e	$0.01 \div 0.2$	eV
D_v	$6 \times 10^{-5}e^{-E_v^m/T}$	m²/s
D_i	$10^{-7}e^{-E_i^m/T}$	m²/s
c_{0v}	$e^{-E_v^f/T}$	–
ω_D	1.11×10^{13}	s⁻¹
r_0	1.5×10^{-9}	m
$\varepsilon_v, \varepsilon_i$	0.1, 0.01	–
ρ_N	10^{12}–10^{15}	m⁻²
Ω	1.206×10^{-29}	m³
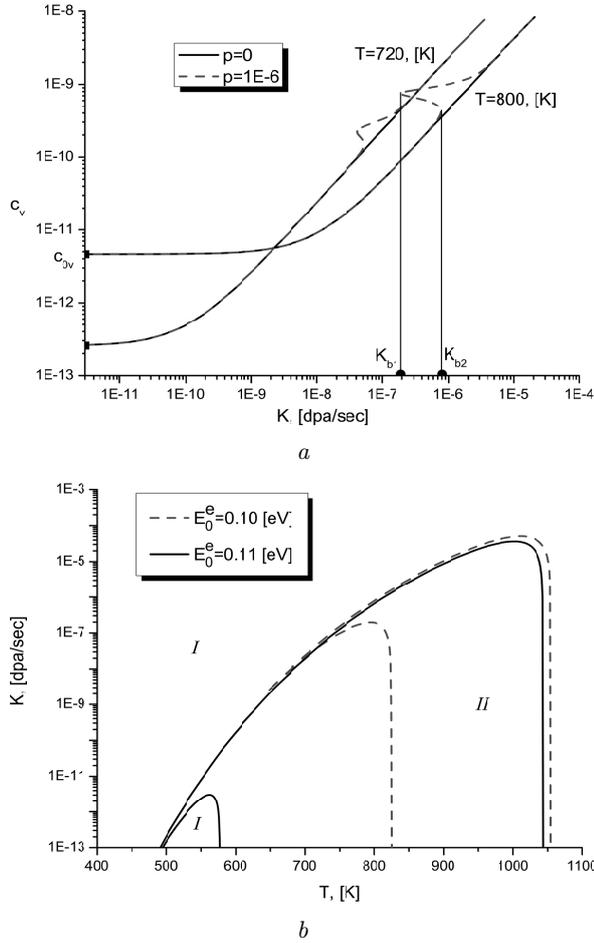
Fig. 2. Stationary dependences of the vacancy concentration at $E_0^e = 0.1$ eV and various temperatures and p (*a*). Phase diagram illustrating the existence of the bimodal mode at $p = 10^{-6}$ and various energies E_0^e (*b*). The dislocation density $\rho_N = 10^{14}$ m^{-2}. The other parameters are quoted in Table 1

results in the formation of nonequilibrium vacancies. The latter, when achieving a certain number corresponding to K_{b2}, bring about the formation of an elastic field that is capable of accelerating the rate of vacancy formation. At this point, the number of vacancies increases drastically and is characterized by a jump in their concentration. If the irradiation dose grows further, the elastic fields cannot strongly affect the processes of defect generation in comparison with cascades, which become a more effective factor at higher rates of dose accumulation. Therefore, at high doses, the corresponding dependence of the vacancy concentration tends to the reference one, which

is obtained provided no influence of the elastic field on the process of vacancy generation.

Hence, it follows from the aforesaid that the system is in a bistable mode in the range of values $K \in [K_{b1}, K_{b2}]$. Binodals, which the values K_{b1} and K_{b2} belong to, form a phase diagram in the plane of independent parameters "damage rate–temperature". The diagram is determined by consistently solving the following two equations:

$$R(x_s; K, T) = 0, \qquad \left.\frac{\partial R(x; K, T)}{\partial x}\right|_{x=x_s} = 0. \qquad (9)$$

The corresponding result is depicted in Fig. 2, *b*. In the beak-shaped region II confined by the binodals, the bistable mode is realized. Regions beyond region II and marked as I correspond to unimodal stationary states with low (at small K's) and high (at large K's) concentrations of defects. It should be noted that an increase of the probability p even by an order of magnitude substantially expands the bimodality region toward low temperatures by lowering the critical value for K. Such a scenario is typical of the irradiation with laser pulses, when the influence of the elastic field is considerable. While comparing the diagrams calculated for different E_0^e-values – actually, they correspond to different mechanical loadings on the system – we obtain a similar scenario, when the temperature interval of the bistability region broadens and the critical value of the dose, at which this mode becomes possible owing to the reduction of the potential barrier for the defect formation and the effective growth of the elastic field energy, diminishes.

Let us analyze the stability of stationary states with respect to small perturbations in the case of non-uniform system. The small deviation $\delta x = x - x_s$ from the uniform stationary state x_s satisfies the equation

$$\partial_t \delta x = (\Lambda(x_s) + \omega(k; x_s))\,\delta x, \qquad (10)$$

where the stability of uniform state with respect to uniform perturbations is given by the index

$$\Lambda(x_s) = -\mu - \frac{P(1 - \varepsilon_i)\epsilon\,\mu\,(1 + B)}{(\mu + \mu B + x_s\epsilon)^2} +$$

$$+ G\frac{\varepsilon(1 - x_s^2)}{(1 + x_s^2)^2}\exp\left(\frac{\varepsilon x_s}{1 + x_s^2}\right), \qquad (11)$$

and the stability with respect to non-uniform perturbations is characterized by the dispersion relation

$$\omega(k; x_s) = -k^2[1 - \varepsilon x_s(1 - \ell^2 k^2)]. \qquad (12)$$

Then, it follows that unstable modes with $\omega(k) > 0$ are characterized by the wave numbers k's ($0 < k < k_c$), where the critical value

$$k_c = \sqrt{\frac{\varepsilon x_s - 1}{\varepsilon x_s \ell^2}} \qquad (13)$$

is determined by the condition $\omega(k) = 0$. In the simplest case with $\ell \to 0$ in the phase diagram region beyond the beak-shaped one, all states with $x_s > 1/\varepsilon$ are unstable with respect to non-uniform perturbations with $k_c \to \infty$, whereas the states with concentrations $x_s < 1/\varepsilon$ are stable. In the sought case with $\ell \neq 0$, the system states with $x_s > 1/\varepsilon$ become unstable, and the corresponding values of wave numbers fall within the interval $0 < k < k_c$. In the bimodality region, the uniform system states are always unstable in respect to non-uniform perturbations. The wave number k_0 corresponding to the most unstable mode can be obtained by solving the equation $d\omega(k)/dk = 0$ and is equal to $k_0 = k_c/\sqrt{2}$.

The results of calculations for the dependences of the critical wave number are exhibited in Fig. 3, *a*. One can see that, in the standard case $p = 0$, the critical wave number grows from zero ($k^* = 0$), when the dose accumulation rate increases from a definite critical value K_c. This means that, when crossing this threshold, there emerge spatial patterns in the system characterized by the infinite period. A further dose accumulation gives rise to the emergence of new patterns, the distance between them decreases, and, at high doses, the period of their arrangement diminishes to about 10^{-8} m. In the case $p \neq 0$, owing to the hysteretic behavior of the stationary concentration, we obtain a scenario when the first unstable mode appears with a nonzero wave number, $k^* = k_c$, at $K > K_{b1}$. The emergence of spatial patterns in the bimodal region of the phase diagram depicted in Fig. 3, *b* occurs in a vicinity of the stationary value c_v corresponding to a metastable state with high concentration; at the same time, no spatial defect patterns are formed in a vicinity of the states with low vacancy concentrations. At elevated temperatures (in the bimodality region), the uniform state loses its stability at larger wave number values and higher damage rates. The critical temperature and dose values,
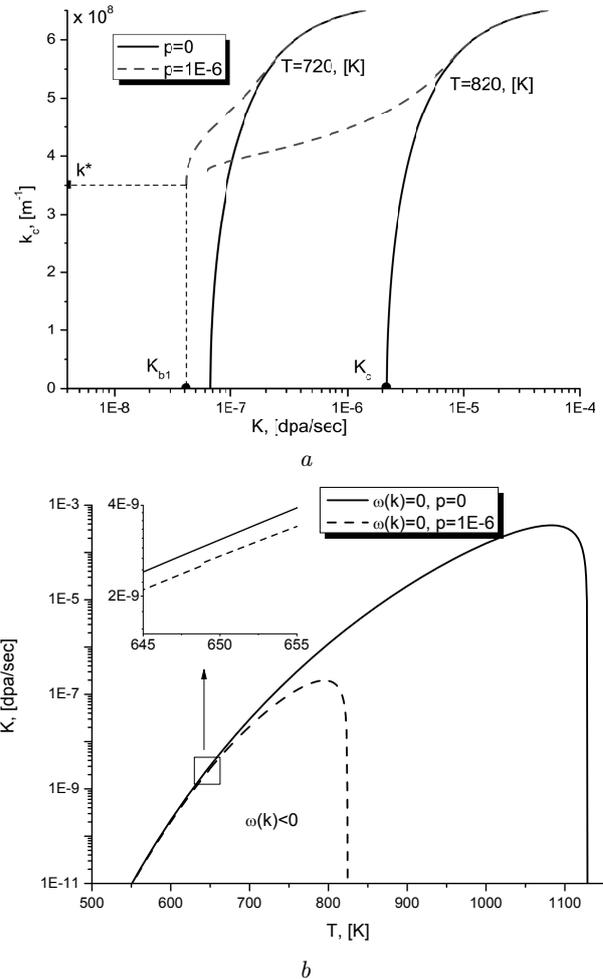
Fig. 3. (*a*) Dependences of the critical wave number on the dose accumulation rate at various p and T. (*b*) Stability diagram calculated in the linear approximation

which confine the regions of existence of spatial defect patterns at $p \neq 0$, are shown in Fig. 3, *b* by dashed curves. The critical K_c and temperature values calculated for $p = 0$ are depicted by a solid curve. In the region above the dashed curves, as well as in the corresponding beak-shaped regions, the processes of pattern formation take place. At $p = 0$, patterns emerge in the region above the thin curve.

4. Influence of Internal-Fluctuation Source

The deterministic model described above is known to be idealized, because it does not take into account the contribution of a fluctuation source that simulates the

influence at the microscopic level on the dynamics of a system. In contrast to the external noise induced by the fluctuations of the environment parameter, the internal noise is induced by the microscopic character of the system itself, with its sources being the internal processes running in the system. Therefore, in what follows, we consider the Langevin dynamics, including the internal noise that is responsible for the dissipative dynamics of the whole ensemble. Certainly, this noise has to be essentially coupled with the validity of the fluctuation-dissipation theorem. Hence, following the standard procedure, let us rewrite the deterministic equation for the concentration field in the form

$$\partial_t x = R(x) + \nabla \cdot M(x)\nabla\mu, \quad \mu \equiv \frac{\delta\mathcal{F}}{\delta x}, \tag{14}$$

where the free energy functional is defined as follows:

$$\mathcal{F}[x] = \int d\mathbf{r} \left[x \ln x - x - \frac{\varepsilon}{2}x^2 + \frac{\varepsilon\ell^2}{2}(\nabla x)^2 \right]. \tag{15}$$

Formally, Eq. (14) can be rewritten in the canonical form within the relaxation model with nonconserved dynamics,

$$\partial_t x = -\frac{1}{M(x)}\frac{\delta\mathcal{U}}{\delta x}, \tag{16}$$

where only the first variational derivative for the functional $U[x]$ is known, i.e.

$$\delta\mathcal{U} = -\int d\mathbf{r}\,\delta x\,[M(x)R(x) + M(x)\nabla\cdot(M(x)\nabla\mu)]. \tag{17}$$

Following works [31, 33, 34], it is possible to introduce a fluctuation source that satisfies the fluctuation-dissipation theorem. In this case, the Langevin dynamics will be described by the equation

$$\partial_t x = -\frac{1}{M(x)}\frac{\delta\mathcal{U}}{\delta x} + \sqrt{\frac{1}{M(x)}}\xi(\mathbf{r}, t), \tag{18}$$

where ξ is a white Gaussian noise with standard properties

$$\langle\xi(\mathbf{r}, t)\rangle = 0, \quad \langle\xi(\mathbf{r}, t)\xi(\mathbf{r}', t')\rangle = 2\sigma^2\delta(\mathbf{r} - \mathbf{r}')\delta(t - t'), \tag{19}$$

and σ^2 is a noise intensity proportional to the temperature.

The influence of such multiplicative noise on system's dynamics at initial stages (in the linear approximation) is analyzed with respect to the stability of concentration fluctuations $\langle\delta x\rangle = \langle x\rangle - x_s$ averaged over the noise, where, as before, x_s is the stationary uniform state of the deterministic system. In the framework of the Stratonovich interpretation of Eq. (18), the evolution of the average concentration-field value is described by the equation

$$\partial_t\langle x\rangle = \langle R(x) + \nabla\cdot M(x)\nabla\mu\rangle - \sigma^2 \left\langle \frac{1}{M^2(x)}\frac{dM(x)}{dx} \right\rangle. \tag{20}$$

Linearizing this equation, we obtain

$$\partial_t\langle\delta x\rangle = \left[\widetilde{\Lambda}(x_s) + \omega(k; x_s) \right]\langle\delta x\rangle, \tag{21}$$

where the indicator of stability with respect to uniform perturbations is determined in terms of its deterministic analog and a term describing the influence of noise. The latter looks like

$$\widetilde{\Lambda}(x_s) = \Lambda(x_s) + \frac{2\sigma^2}{x_s^3}. \tag{22}$$

From whence, it follows that the internal noise makes a positive contribution to the Lyapunov indicator, i.e. to the destabilization of the uniform state at early stages of evolution of the system.

While studying the behavior of the system in the stationary case, the major quantity is the stationary distribution of the concentration field, $\mathcal{P} \equiv \mathcal{P}_s([x], t \to \infty)$, which is a solution of the Fokker–Planck equation [35]. The latter, according to the Langevin equation (18), reads

$$\partial_t\mathcal{P} = \int d\mathbf{r}\frac{\delta}{\delta x}\left[\frac{1}{M(x)}\left(\frac{\delta\mathcal{U}}{\delta x} - \sigma^2\frac{1}{M(x)}\frac{dM(x)}{dx} \right)\mathcal{P} + \right.$$

$$\left. + \sigma^2\frac{\delta}{\delta x}\frac{1}{M(x)}\mathcal{P} \right]. \tag{23}$$

Its exact solution, provided no probability density flux across the boundaries, which is considered natural, has a quasi-Gibbs form,

$$\mathcal{P}_s[x] \propto \exp(-\mathcal{F}_{\text{ef}}[x]/\sigma^2), \tag{24}$$

where the effective functional of free energy consists of the initial functional, which plays the role of internal energy, and the entropy contribution times the

effective temperature, the latter being reduced to the renormalized noise intensity Σ,

$$\mathcal{F}_{\text{ef}}[x] = \mathcal{U}[x] - \Sigma\mathcal{S}_{\text{ef}}[x], \quad \mathcal{S}_{\text{ef}}[x] \equiv \int d\mathbf{r} \ln M(x). \ (25)$$

Here, $\mathcal{S}_{\text{ef}}[x]$ is the effective entropy expressed in terms of the mobility $M(x)$. Hence, it follows that the internal noise can essentially change the states of a stationary system owing to the entropic contribution by changing the number of extrema in the stationary distribution of the concentration field at fixed key parameters of the system. The corresponding qualitative transformations with the emergence of the so-called "macroscopic phases" (they are determined by the maxima in the probability density) and transitions between them (they are initiated by a change of the effective entropy) are known as entropy-driven phase transitions (see, e.g., works [33, 34, 36–40]). For systems with the conserved dynamics, those phase transitions bring about the phase separation [38, 41] or, in general, pattern formation [33, 34, 37]. Below, we are interested in the latter case, which makes it possible to describe the character of stationary point-defect patterns that emerge under the action of the constant irradiation.

In order to study the processes of pattern formation at later time intervals – namely, in the stationary case – it is enough to solve the Cauchy problem, while minimizing the functional of effective free energy, the minima of which correspond to the probability density maxima in the distribution of the defect concentration field and, hence, to the most probable spatial configurations of point defects. Therefore, from the mathematical viewpoint, the problem is reduced to the solution of the equation for the most probable structures, whose evolution, as was demonstrated earlier (see, e.g., works [31, 42]), is described by the equation

$$\partial_t x = -\frac{1}{M(x)} \frac{\delta \mathcal{F}_{\text{ef}}[x]}{\delta x}, \tag{26}$$

and the relevant periodic boundary conditions. Its solutions are stationary patterns $x_s(\mathbf{r}, t \to \infty)$, the morphology of which will be studied with the help of nonlinear analysis. Substituting the corresponding definitions, we arrive at the equivalent equation

$$\partial_t x = R_{\text{ef}}(x) + \nabla \cdot M(x)\nabla\mu,$$

$$R_{\text{ef}}(x) \equiv R(x) + \frac{\Sigma}{M^2(x)} \frac{dM(x)}{dx}. \tag{27}$$
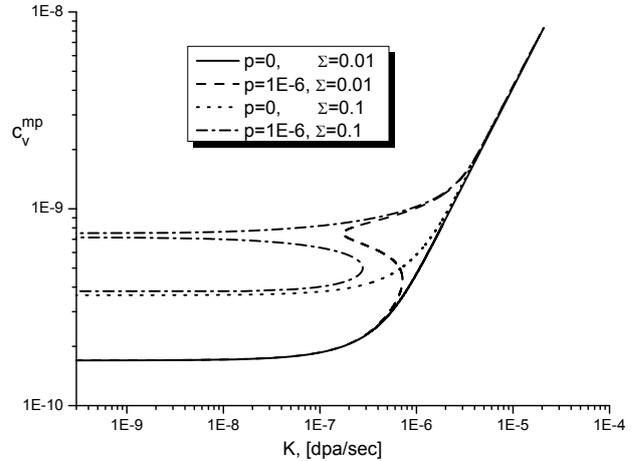
Fig. 4. Dependences of the most probable values of vacancy concentration on the dose accumulation rate at $T = 800$ K, $E_0^e = 0.01$ eV, and for various intensities of the internal noise

From it, one can see that the Stratonovich drift acts oppositely to its contribution at short time intervals obtained when the system stability is analyzed in the linear approximation [31, 42]. From the physical viewpoint, this situation is a manifestation of the Le Chatelier principle. The corresponding scenario is inherent to the systems that undergo entropy-driven phase transitions, the latter being considerably different from nonequilibrium transitions with external noise [36, 39, 40, 43].

Let us consider the character of noise-induced variations in the most probable states by neglecting the spatial component in Eq. (27). In this case, instead of the functional $\mathcal{P}_s[x]$, we have the distribution function $P_s(x)$, and the solutions of the equation $R_{\text{ef}}(x) = 0$ determine the positions of its extrema, x_{mp}. The dependences of the most probable concentration values, c_v^{mp}, at various noise intensities Σ are shown in Fig. 4. One can see that noise stimulates the growth of the stationary, most probable concentration and substantially expands the bistability region. Thus, noise enhances the contribution of elastic fields, if any, due to the stochastic generation of defects.

5. Features of the Stationary Pattern Formation in a Nonlinear System

In order to analytically analyze the processes of stationary pattern formation in nonlinear systems, let us consider the behavior of the unstable mode am-
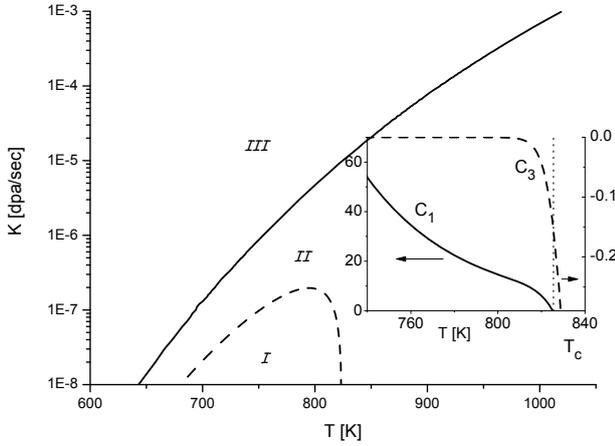
Fig. 5. Diagram of the pattern formation in the one-dimensional case and at $p = 10^{-6}$. The inset shows the expansion coefficients $\mathcal{C}_1$ and $\mathcal{C}_3$ calculated for $K = 10^{-6}$ d.p.a/s and $\Sigma = 0$

plitude in the framework of the standard approach [8]. For this purpose, we will confine the analysis to the one-dimensional case, which can provide us with a basic information concerning the possibility of formation of stationary defect patterns. Let us linearize the right-hand side of Eq. (27) with respect to an independent parameter, the temperature, in a vicinity of the critical temperature T_c, above which the spatial patterns are formed at a fixed dose accumulation rate K. In this case, the expression for the effective reaction component in the dynamics of the most probable concentration values looks like

$$\mathcal{R} = R_{\text{ef}}(x, T_c) + \left.\frac{\mathrm{d}R_{\text{ef}}(x,T)}{\mathrm{d}T}\right|_{T=T_c} (T - T_c). \qquad (28)$$

The main attention will be concentrated on the instabilities that arise in a vicinity of the uniform, most probable states x_{mp}; the latter can be determined by solving the equation $R_{\text{ef}}(x_{mp}, \varepsilon) = 0$. For the sake of simplicity, let us first consider the one-dimensional case ($\mathbf{r} \to \rho$). By introducing the scale $\alpha^2 = T - T_c$, let us examine the case of instabilities with the wave number k characterized by the width $\mathcal{O}(\alpha)$ and the instability order $\mathcal{O}(\alpha^2)$. For further purposes, we use the auxiliary field $w(\rho,t) \equiv (x(\rho,t) - x_{mp})$, where

$$w(\rho,t) = \alpha\phi(\rho,t) \equiv \alpha A(\varrho,\tau)e^{ik\rho} + \text{c.c.}$$

is expressed in terms of a slow amplitude $A(\varrho,\tau)$. In the one-dimensional case, only the pair of critical wave numbers $(k_1, -k_1)$ is possible, $\varrho = \alpha\rho$,

and $\tau = \alpha^2 t$. The notation c.c. means the complex conjugation. We should expand $\mathcal{R}$ in a series in $\alpha\phi = x - x_{mp}$,

$$\mathcal{R}(\alpha\phi) \simeq \mathcal{A}_1\alpha\phi + \mathcal{A}_2(\alpha\phi)^2 + \mathcal{A}_3(\alpha\phi)^3;$$

$$\mathcal{A}_n = \frac{1}{n!}\left.\frac{\mathrm{d}^n\mathcal{R}}{\mathrm{d}x^n}\right|_{x=x_{mp}}. \qquad (29)$$

Using the relations $\partial_t \to \alpha^2\partial_\tau$ and $\nabla \to (ik + \alpha\partial_\varrho)$, substituting $w(\rho,t)$ into Eq. (27), and comparing the coefficients at every $\alpha^n e^{ink\rho}$ (for available n's), we arrive at the equation for the unstable amplitudes in the form

$$\partial_\tau A = \mathcal{C}_1 A + \mathcal{C}_3|A|^2 A + \partial_\varrho^2 A, \qquad (30)$$

where the expansion coefficients are

$$\mathcal{C}_1 \equiv \left.\frac{\mathrm{d}^2 R_{\text{ef}}(x,T)}{\mathrm{d}x\mathrm{d}T}\right|_{x=x_{mp},T=T_c} + x_{mp}k^2(1 - \ell^2 k^2),$$

$$\mathcal{C}_3 \equiv \frac{1}{3!}\left.\frac{\mathrm{d}^3 R_{\text{ef}}(x,T_c)}{\mathrm{d}x^3}\right|_{x=x_{mp}}. \qquad (31)$$

The derived equation belongs to the class of equations with the spatial operator of the Swift–Hohenberg type [8, 44]. In the case $\mathcal{C}_1 < 0$ and $\mathcal{C}_3 < 0$, the trivial value of hydrodynamic mode amplitude ($A = 0$) is realized, which means the absence of a spatial defect ordering, i.e. we obtain a uniform (chaotic) distribution of point defects over the system. The pattern formation becomes possible only if $\mathcal{C}_1 > 0$ and $\mathcal{C}_3 < 0$. Then, the family of stationary solutions $A_k = |A_k|e^{i\psi}$ has the amplitudes $|A_k| = \sqrt{\mathcal{C}_1/|\mathcal{C}_3|}$, and the phase ψ is arbitrary.

The pattern formation diagram in the one-dimensional case at $p = 10^{-6}$ is depicted in Fig. 5. Here, making allowance for the linear analysis of stability, three characteristic regions with respect to the $\mathcal{C}_1$- and $\mathcal{C}_3$-values can be distinguished. Region I restricts the temperature and dose accumulation rate values, for which the uniform distribution of defects is stable. Beyond it, the uniform distribution of defects is unstable. Region III is characterized by the condition $\mathcal{C}_1 > 0$ and $\mathcal{C}_3 < 0$. Here, according to the results of nonlinear analysis, T and K have the values, at which patterns are stationary. Evidently, in region II, arising instabilities do not form stationary defect patterns; the latter have a transient character. In other words, they disappear after a long

enough time of the evolution of the system. In the two-dimensional case, region III becomes so expanded that the region of transient patterns degenerates, and only regions I and III survive. For a system with $p = 0$, only regions I and III with no transient patterns can be distinguished. In the both cases, noise gives rise to a reduction of $\mathcal{C}_3$ at small x_{mp} owing to the contribution $-(\Sigma/4)x_{mp}^5$ to the deterministic component $\mathcal{C}_3$. Hence, the internal noise can substantially expand the stationary pattern formation region even at low defect concentrations.

6. Simulation

In order to verify the results of analytical calculations, let us carry out a numerical simulation using a mesh with square (cubic) symmetry, which corresponds to the nickel structure, and taking advantage of a finite-difference scheme. Assuming no anisotropy, the mesh step is selected to equal $\Delta l =$ $= 0.5$. Since $L_d = \rho_N^{-1/2}$, we obtain $L_d = 10^{-7}$ m for $\rho_N = 10^{14}$ m^{-2}. The number of mesh points in both spatial directions is $N = 128$. In this case, the total length of the system in either direction amounts to $L = 25L_d$. For the length scale, we put $\ell = 0.25$, which automatically means that $r_0 = 2.5 \times 10^{-8}$ m. The boundary conditions are chosen periodic. As the initial condition, we select the equilibrium value of vacancy concentration, i.e. $\langle x(\mathbf{r}, 0) \rangle = x_0$ with a 10%-spread of values around the average one. To ensure the stability of a numerical simulation algorithm, the time increment is taken equal to $\Delta t = 10^{-4}$, which corresponds to the physical time interval of the cascade relaxation.

A typical picture of evolution with the formation of defect pores is illustrated in Fig. 6. Here, the dark regions correspond to the phase with a depleted defect density, whereas the light ones to the defect-enriched phase. One can see from the figure that, proceeding from a chaotic configuration of defects, the extended defect patterns are first formed in the system within a short time interval; then they decay into small aggregates (pores) that are more stable at the given irradiation parameters. The corresponding dynamics demonstrates effects of the vacancy attachment to extended defects and their decay into separate pores. This process is weakly pronounced, but it can be observed in statistical characteristics in the form of oscillations.
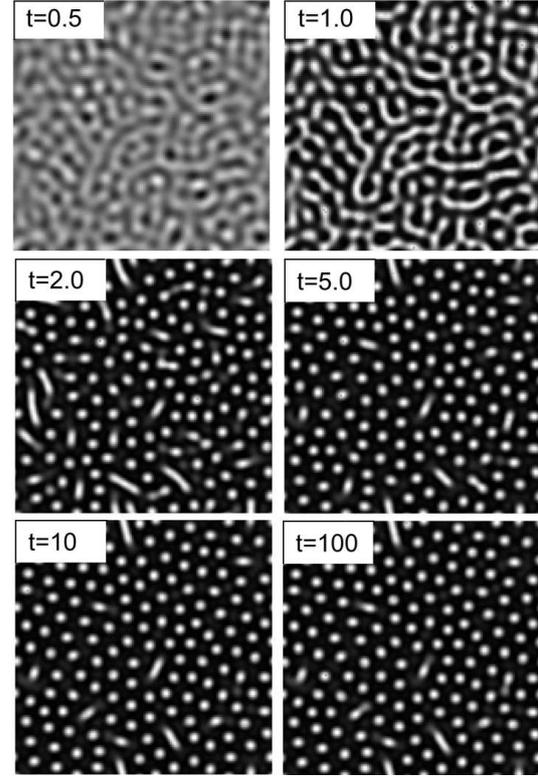

Fig. 6. Typical scenario of the defect pattern formation in the form of pores at $T = 778$ K, $K = 10^{-6}$ d.p.a/s, $E^e = 0.1$ eV, $p = 10^{-6}$, and $\Sigma = 0.001$

To describe the formation of patterns with the distribution of the defect density in clusters, we use the average defect density m_1, the dispersion of the defect density spread m_2, the asymmetry m_3, and the excess m_4 defined in the standard way:

$$m_1 = \langle x \rangle; \quad m_2 = \langle (x - \langle x \rangle)^2 \rangle;$$
$$m_3 = \frac{\langle (x - \langle x \rangle)^3 \rangle}{m_2^3}, \quad m_4 = \frac{\langle (x - \langle x \rangle)^4 \rangle}{m_2^4}, \quad (32)$$

where m_2 determines the width of the intermediate layer between two phases (defect-depleted and defect-enriched ones). The asymmetry parameter evaluates the profile symmetry for the defect distribution at the basic level. Its sign characterizes the position of generating points proportionally in the defect-enriched ($m_3 > 0$) or defect-depleted ($m_3 < 0$) phase in comparison with the average level of the defect distribution. The excess parameter describes the distribution stochasticity in comparison with the perfectly
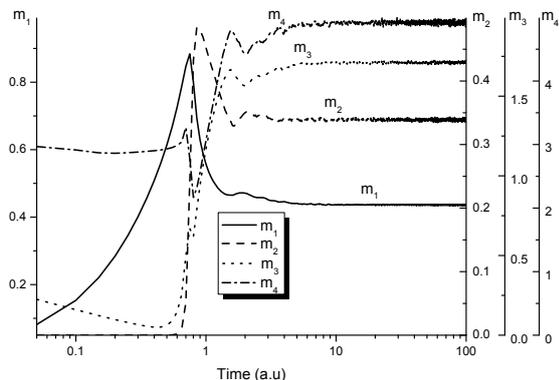
Fig. 7. Dynamics of the average value (solid curve), dispersion (dashed curve), asymmetry (dotted curve), and excess (dash-dotted curve) parameters at $T = 778$ K, $K = 10^{-6}$ d.p.a/s, $E^e = 0.1$ eV, $p = 10^{-6}$, and $\Sigma = 0$
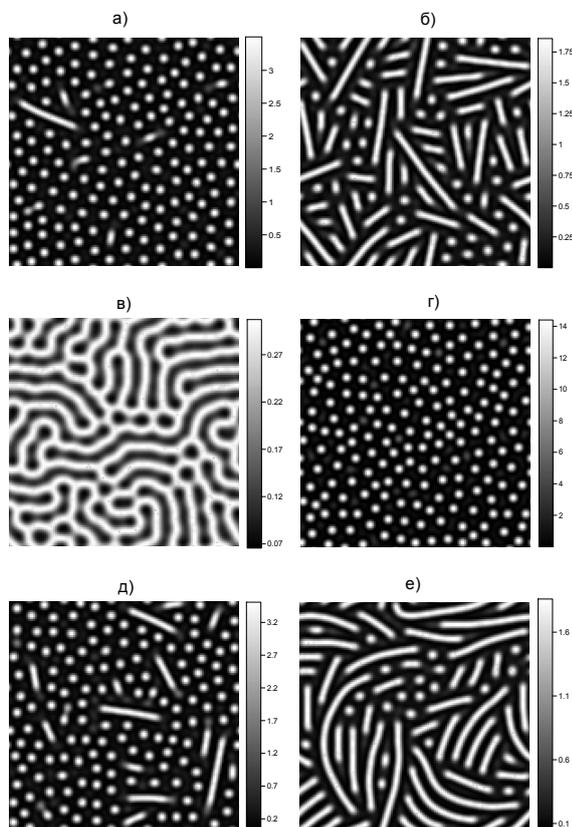

Fig. 8. Typical stationary defect patterns obtained at the dose accumulation rate $K = 10^{-6}$ d.p.a/s and various $T =$ $= 730$ (a), 773 (b), and 825 K (c), and at $K = 10^{-5}$ d.p.a/s and $T = 773$ K (d); the exhibited patterns correspond to the deterministic case. Structures (e) and (f) were obtained at $K = 10^{-6}$ d.p.a/s, $\Sigma = 0.01$, and $T = 730$ (e) and 773 K (f)

chaotic (Gaussian) distribution ($m_4 = 3.0$ for the Gaussian distribution). This parameter also characterizes a nonsmoothness of the distribution function for x. If the majority of peculiarities (excitations in the defect-enriched phase) are concentrated near the average level, the excess value is less than in the case where they are located far from this level. The average defect density m_1 can grow, but it gives no information concerning the character of the pattern formation. The relevant information is provided by the dispersion m_2; namely, its growth testifies to the emergence of new phases, defect-enriched and defect-depleted ones. The asymmetry and excess parameters describe how much those phases are different.

The results of simulation showed that, for a completely chaotic distribution of defects in the crystal characterized by an equilibrium defect concentration, we have the following dynamics of pattern formation (see Fig. 7). At short time intervals, the defects are accumulated to a level sufficient for their spatial organization. At this stage, the dispersion is close to zero, which testifies to the absence of interfaces between two phases. After the maximum in the dependence $m_1(t)$ is reached, the dispersion starts to grow, which reflects an ordering in the system; the defects start to attract one another and aggregate into clusters. At this stage, the asymmetry starts to substantially deviate from zero, and the excess from a value of 3. It is significant that a weak excess and asymmetry oscillations testify to the oscillatory character of the extended defect growth: the attachment of defects to and their emission from clusters. The reduction in the number of accumulated defects distributed over the crystal testifies to their migration to sinks, namely, pores. If the irradiation time grows further, a stationary mode is established, when the statistical moments do not change. It should be noted that, in the range of dose accumulation rate or temperature, when we are in the region below the curves describing the loss of stability in the uniform distribution (see Fig. 3, b), the average value gradually grows without manifestating a peak, whereas the dispersion is constant and equal to zero, which testifies that the emergence of defect patterns under such conditions is impossible (the corresponding dependences, being trivial, are not presented).

Let us consider the stationary patterns that arise at various temperature or dose accumulation regimes separately (see Fig. 8). From the presented results,
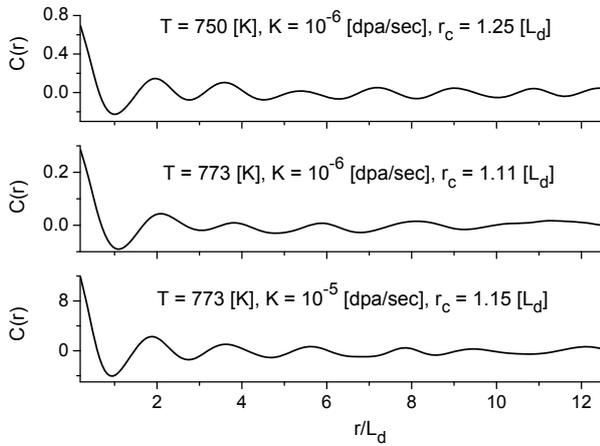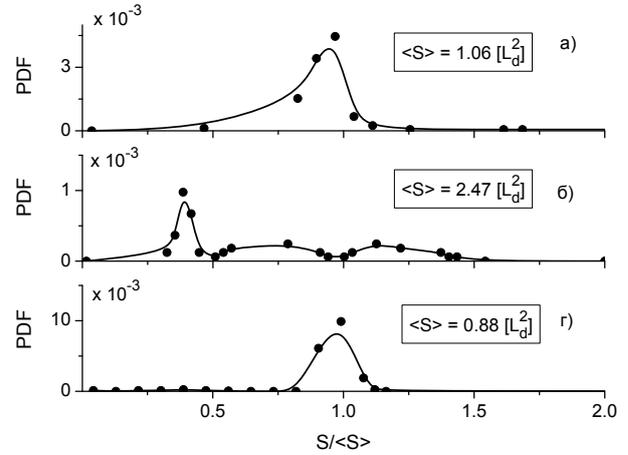
Fig. 9. Spherically averaged correlation functions for various relationships between the irradiation temperature and the dose accumulation rate
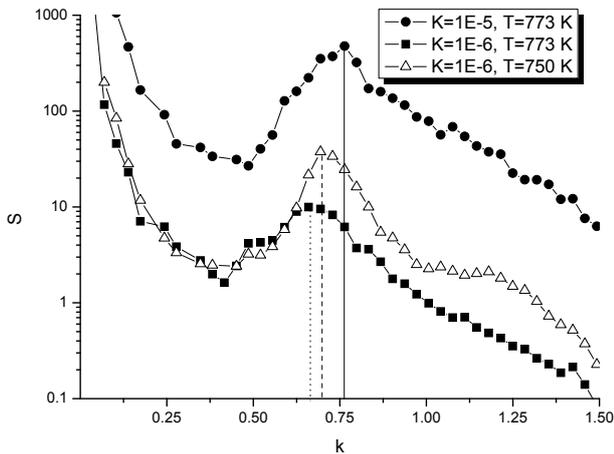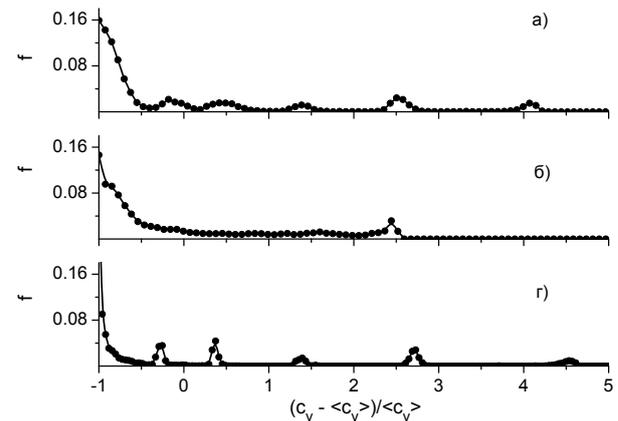

Fig. 10. Behavior of the spherically averaged structural factor in the stationary case for various temperatures and dose accumulation rates

Fig. 11. Distribution functions over the pore dimensions at $T = 750$ K and $K = 10^{-6}$ d.p.a/s (the upper panel), $T = 773$ K and $K = 10^{-6}$ d.p.a/s (the middle panel), and $T = 773$ K and $K = 10^{-5}$ d.p.a/s (the lower panel)

Fig. 12. Distribution functions over the vacancy concentration in clusters at $T = 750$ K and $K = 10^{-6}$ d.p.a/s (the upper panel), $T = 773$ K and $K = 10^{-6}$ d.p.a/s (the middle panel), and $T = 773$ K and $K = 10^{-5}$ d.p.a/s (the lower panel)

it follows that, at low temperatures and dose accumulation rates (see Fig. 8, *a*), the vacancy clusters emerge in the system. Some clusters are extended defects; for instance, it can be a self-intersection of a vacancy loop in the three-dimensional space or an intersection of defect walls. At elevated temperatures, the number of extended defects considerably grows (see Figs. 8, *b* and *c*). The defect concentration decreases at that, and, when approaching the line of stationary pattern existence, defects are smeared out over the whole system. It is significant that, when the dose accumulation rate increases, the spherical

aggregates of defects mainly appear, and the number of defects in pores considerably grows (see Fig. 8, *d* and the distribution of *x*-values in every panel). The stationary patterns which are the most probable at $\Sigma = 0.01$ are depicted in Figs. 8, *e* and *f*. From all that, one can see that, in the stationary case, the internal noise stimulates the formation of extended defects.

Let us carry out the correlation analysis of the described stationary patterns. For this purpose, we should determine the properties of the two-point,

one-time spherically averaged correlation function $\langle \delta x(0,t) \delta x(r,t) \rangle$, where $\delta x = x - \langle x \rangle$. Its typical dependences for various relationships between the temperature and the dose accumulation rate are shown in Fig. 9. In the general case, the correlation function can be approximated by the dependence $C(r) = C(0)e^{-r/r_c} \sin(2\pi r/\langle r_0 \rangle + \phi)$, where r_c is the correlation length, $\langle r_0 \rangle$ the average period of the patterns, and ϕ an arbitrary phase. In our research, we are interested in the dependence of the correlation length on the key parameters of the system, whereas the pattern period will be estimated using the Fourier analysis. From the approximation of correlation functions, it follows that both a decrease in the temperature and an increase in the rate K bring about a reduction of the correlation length (formation of compact spherical defect patterns), with, in general, $r_c \sim 100$ nm. However, at elevated rates K, the correlation length decreases because the lattice pore symmetry becomes violated due to the radiation-stimulated formation of additional pores in the pore lattice. If the temperature grows owing to the formation of extended defects, the correlation length increases. The estimation of the quantity $\langle r_0 \rangle$ shows that its value is comparable with the diffusion length L_d, so that $\langle r_0 \rangle / r_c \sim 10^{-1}$. While studying the pattern period, an important quantity is the spherically averaged structural factor $S(k,t) = N^{-2} \sum_{k<|\mathbf{k}|<k+\Delta k} S(\mathbf{k},t)$, where $S(\mathbf{k},t)$ is the structural factor determined using the Fourier transformation of the correlation function depending on the vector argument, $C(\mathbf{r})$, and Δk is the ring width in the reciprocal space. The corresponding dependences for $S(k)$ are exhibited in Fig. 10. The figure demonstrates that the position of the main peak, which determines the pattern period, completely agrees with the results of the linear analysis carried out above for the stability of the system. Really, the peak shifts toward larger wave numbers at higher dose accumulation rates and lower temperatures. In addition, the peak height considerably increases at large K, which testifies to a high degree of ordering in defect patterns.

Now, let us examine the distribution of defect patterns over their dimensions by calculating the corresponding probability distribution function (PDF(S)) over sizes using the simulation data (see Fig. 11). From the results obtained, it follows that, at $T = 750$ K and $K = 10^{-5}$ d.p.a/s, as well as at $T = 773$ K and $K = 10^{-6}$ d.p.a/s, when spherical

clusters are mainly realized, $PDF(S)$ is centered in a vicinity of the average cluster plane, $\langle S \rangle$. The appearance of extra maxima at $T = 773$ K and $K = 10^{-6}$ d.p.a/s is explained by the formation of extended defects giving a contribution to the distribution. It should be noted that, in the case of high dose accumulation rates, the distribution peak grows by an order of magnitude. This circumstance testifies that the pore ensemble is characterized by a small dispersion of pore dimensions, so that $S \approx \langle S \rangle$. In accordance with the calculated values, we have that $\langle S \rangle \sim L_d^2$ for spherical patterns, and $\langle S \rangle$ increases when the extended defect patterns emerge.

At last, let us consider the distribution function of the vacancy concentration in clusters, $f(c_v)$, obtained under various irradiation conditions (see Fig. 12). It should be noted that, in all analyzed cases, the distribution function is not centered in a vicinity of the average concentration $\langle c_v \rangle$. The presence of peaks in the function $f(c_v)$ means the formation of vacancy clusters with different contributions. In the upper panel of Fig. 12, the peak smearing is associated with the presence of extended defects, the number of which is small at $T = 750$ K and the given dose accumulation rate. In the case of elevated temperatures, when the number of extended defects is substantial (the middle panel), the majority of vacancy clusters are characterized by a smeared distribution and a single peak. In the case of higher dose accumulation rates (the lower panel), when all defects are grouped into spherical pores with almost identical dimensions $\langle S \rangle$, the number of defects in the clusters is characterized by a small concentration dispersion (in comparison with the case $T = 750$ K and $K = 10^{-6}$ d.p.a/s).

7. Conclusions

Within the generalized rate theory for the evolution of point defects in irradiated materials and nickel, as an example, the processes of pattern formation for defects of the vacancy type have been studied. The developed model makes allowance for the processes of defect generation by the deformation fields induced by defects themselves, as well as for the interaction between defects. The generalization of the dynamic approach has been carried out by introducing a stochastic evolution component into consideration.

It was found that the action of elastic fields at the stage of defect generation in the examined system can give rise to the formation of bistable states

at low dose accumulation rates, which are characteristic of laser irradiation, and explains the thermofluctuation mechanism of defect formation. The phase diagram was plotted in the plane "dose accumulation rate–temperature", which revealed the region of bimodality existence. While studying the stability of the uniform defect distribution in a crystalline system in the framework of linear analysis, it is shown that the spatial perturbations, which are an impetus for the processes of pattern formation to run, emerge in restricted intervals of working temperatures and dose accumulation rates. In the case of a low dose accumulation rate, the first unstable mode is found to be characterized by a nonzero wave number. In the framework of the linear approximation, it was demonstrated that the period of formed defect patterns (vacancy or pore aggregates) decreases with the growth of the dose accumulation rate and the temperature, the result being in agreement with known literature data (see, e.g., work [11]).

While studying the influence of the stochastic component, which describes the action of microscopic processes of defect formation and defines the statistical character of pattern formation, it is found that, at early stages of system's evolution, this noise leads to the destabilization of the uniform system state, whereas it acts oppositely at later stages. This effect corresponds to the mechanism of entropy-driven phase transitions in stochastic systems with internal multiplicative noise. Therefore, it is necessary to consider the random factors that can considerably affect the dynamics of a system at various stages of its evolution. It is established that this statistical approach makes it possible to analyze the properties of stationary patterns.

While examining the conditions of the stationary pattern formation in the framework of nonlinear analysis (in the case of weakly varying amplitudes in the hydrodynamic mode), it is shown that the character of pattern formation can be described, by using a simple equation for those amplitudes. The results of the relevant research made it possible to plot the phase diagram, which evidences that the emerging patterns can be classed into stationary and transient (with a finite time of existence) ones.

The described approaches are used to carry out a numerical simulation, which allows the changes in the morphology of defect patterns to be studied when the temperature and the rate of dose accumulation vary (within the intervals corresponding to those obtained at irradiation in reactors). It was established that, if a deviation in the phase diagram from the pattern formation region is insignificant, the defects become organized into extended clusters with low vacancy concentrations. As the temperature decreases, the separate vacancy clusters, which can be identified as pores, are formed between the extended defects. If the temperature decreases further or the dose accumulation rate increases, the pores become main structural units. With the help of correlation analysis, it is found that the characteristic dimension of pores is of the order of 100 nm, and the correlation length can be slightly different from this value. The latter circumstance testifies to a periodicity in the arrangement of vacancy-induced pores in nickel, which was confirmed by the results of researches of the structural factor and the distribution function of pores over their dimensions. The results of numerical simulation completely agrees with those of analytical calculations; they qualitatively and quantitatively correspond to the known experimental data obtained for the pattern formation from defects of the vacancy type [11].

Despite that the model discussed in this work does not consider the dynamics of interstitial atoms, which quickly migrate to sinks, and does not include the emission of vacancies from pores (their dynamics is not presented in the evolution equations), the developed approach can be used to study the behavior of defects of the vacancy type not only under irradiation conditions in reactors and laser pulses. It can be applied also to the analysis of the defect formation at irradiation on linear accelerators and when an external mechanical loading is applied to the crystalline system.

1. J.H. Evans, Nature **229**, 403 (1971).
2. S. Saass and B.L. Eyre, Phil. Mag. **27**, 1447 (1973).
3. P.B. Johnson, D.J. Mazey, and J.H. Evans, Radiat. Eff. **78**, 147 (1983).
4. J.E. Evans and D.J. Mazey, J. Nucl. Mater. **138**, 176 (1986).
5. A. Jostobns and K. Farrel, Radiat. Eff. **15**, 217 (1972).
6. J.O. Steigler and K. Farrel, Scr. Metal. **8**, 651 (1974).
7. V.V. Uglov, *Radiation-Induced Effects in Solids* (Belarusian State Univ., Minsk, 2007) (in Russian).
8. D. Walgraef, *Spatio-Temporal Pattern Formation* (Springer, New York, 1996).

9. F.Kh. Mirzoev, V.Ya. Panchenko, and L.A. Shelepin, Usp. Fiz. Nauk **166**, 3 (1996).

10. F.Kh. Mirzoev, and L.A. Shelepin, Pis'ma Zh. Tekhn. Fiz. **22**, No. 13, 28 (1996).

11. V.N. Voevodin and I.M. Neklyudov, *Structural-Phase State Evolution and Radiation Resistance of Structural Materials* (Naukova Dumka, Kiev, 2006) (in Russian).

12. R.Enrique and P.Bellon, Phys. Rev. Lett. **84**, 2885 (2000).

13. R.A. Enrique and P. Bellon, Phys. Rev. E **63**, 134111 (2001).

14. J. Ye and P. Bellon, Phys. Rev. B**70**, 094104 (2004).

15. N. Ofori-Opoku, J.J. Hoyt, and N. Provatas, Phys. Rev. E **86**, 066706 (2012).

16. K.R. Elder and M. Grant, Phys. Rev. E **70**, 051605 (2004).

17. P.F. Tupper and M. Grant, Eur. Phys. Lett. **81**, 40007 (2008).

18. J. Berry, M. Garnt, and K.R. Elder, Phys. Rev. E **73**, 031609 (2006).

19. K.R. Elder, N. Provatas, J. Berry, P. Stefanovich, and M. Grant, Phys. Rev. B **75**, 064107 (2007).

20. A. Jaatinen, C.V. Achim, K.R. Elder, and T. Ala-Nissila, Phys. Rev. E **80**, 031602 (2009).

21. D. Kharchenko, I. Lysenko, and V. Kharchenko, Physica A **389**, 3356 (2010).

22. D.O. Kharchenko, V.O. Kharchenko, and I.O. Lysenko, Cent. Eur. J. Phys. **9**, 698 (2011).

23. D.O. Kharchenko, V.O. Kharchenko, S.V. Kokhan, and I.O. Lysenko, Ukr. J. Phys. **57**, 1069 (2012).

24. D.O. Kharchenko, V.O. Kharchenko, I.O. Lysenko, and S.V. Kokhan, Phys. Rev. E **82**, 061108 (2010).

25. V.O. Kharchenko and D.O. Kharchenko, Cond. Matter Phys. **14**, 23602 (2011)

26. D.O. Kharchenko, A.V Dvornychenko, and I.O. Lysenko, Ukr. J. Phys. **53**, 917 (2008).

27. D.O. Kharchenko, I.O. Lysenko, and V.O. Kharchenko, Ukr. J. Phys. **55**, 1226 (2010).

28. P.K. Galenko, D. Kharchenko, and I. Lysenko, Physica A **389**, 3443 (2010).

29. G. Martin, Phys. Rev. B. **30**, 1424 (1984).

30. C. Abromeit and G. Martin, J. Nucl. Mater. **271–272**, 251 (1999).

31. V.O. Kharchenko and D.O. Kharchenko, Eur. Phys. J. B **85**, 383 (2012).

32. D. Batogkh, M. Hildebrant, F. Krischer, and A. Mikhailov, Phys. Rep. **288**, 435 (1997).

33. D.O. Kharchenko, S.V. Kokhan, and A.V. Dvornichenko, Physica D **238**, 2251 (2009).

34. S.E. Mangioni and H.S. Wio, Phys. Rev. E **71**, 056203 (2005).

35. H. Risken, *The Fokker-Planck Equation* (Springer, Berlin, 1984).

36. M. Ibanes, J. Garcia-Ojalvo, R. Toral, and J.M. Sancho, Phys. Rev. Lett. **87**, 020601 (2001).

37. K. Wood, J. Buceta, and K. Lindenberg, Phys. Rev. E. **73**, 022101 (2006).

38. D.O. Kharchenko and A.V. Dvornichenko, Physica A **387**, 5342 (2008).

39. D.O. Kharchenko and A.V. Dvornichenko, Eur. Phys. J. B **61**, 95 (2008).

40. V.O. Kharchenko, Physica A **388**, 268 (2009).

41. D.O. Kharchenko, I.O. Lysenko, and S.V. Kokhan, Eur. Phys. J. B. **76**, 37 (2010).

42. S.E. Mangioni, Physica A **389**, 1799 (2010).

43. J. Buceta and K. Linderberg, Phys. Rev. E **69**, 011102 (2004).

44. P.C. Hohenberg and B.I. Halperin, Rev. Mod. Phys. **49**, 435 (1997).

Д.О. Харченко, В.О. Харченко, А.І. Баштова

МОДЕЛЮВАННЯ ПРОСТОРОВОЇ
ОРГАНІЗАЦІЇ ТОЧКОВИХ ДЕФЕКТІВ
В ОПРОМІНЮВАНИХ СИСТЕМАХ

Р е з ю м е

Запропоновано узагальнений статистичний підхід до опису процесів організації точкових дефектів вакансійного типу у кластери та пори на прикладі нікелю в рамках швидкісної теорії, що враховує генерацію дефектів пружними полями та взаємодію дефектів. Проведено дослідження умов виникнення структур дефектів у робочих режимах опромінення в реакторах. Встановлено характер зміни мікроструктури при різних температурах та швидкостях набору дози в рамках використання аналітичних підходів та методів числового моделювання. Досліджено зміну періоду структур та їх характерних розмірів за допомогою статистичного аналізу даних моделювання. Отримані результати узгоджуються з експериментальними спостереженнями за процесами дефектоутворення при опроміненні в реакторних умовах.